

PRESSURE CYCLING OF TYPE 1 PRESSURE VESSELS WITH GASEOUS HYDROGEN

San Marchi, C.¹, Dedrick, D.E.¹, Van Blarigan, P.¹, Somerday, B.P.¹ and Nibur, K.A.²

¹ Sandia National Laboratories, 7011 East Ave, Livermore CA 94550, USA

² Hy-Performance Materials Testing, LLC, Bend OR, USA

ABSTRACT

Type 1 steel pressure vessels are commonly used for the transport of pressurized gases, including gaseous hydrogen. In the majority of cases, these cylinders experience relatively few pressure cycles over their lifetime, perhaps in the hundreds. In emerging markets, such as hydrogen-powered industrial trucks, hydrogen fuel systems are expected to experience thousands of cycles over just a few year period. This study investigates the fatigue life of Type 1 steel pressure vessels by subjecting full-scale vessels to pressure cycles with gaseous hydrogen between nominal pressure of 3.5 and 43.8 MPa. In addition, engineered defects were machined on the inside of several pressure vessels for comparison to fatigue crack growth measurements on materials sectioned from these pressure vessels. As-manufactured pressure vessels have sustained >35,000 cycles with failure, while vessels with machined defects leaked before bursting after 8,000 to 15,000 pressure cycles. The measured number of cycles to failure in these pressure vessels is two to three times greater than predicted using conservative methods based on fatigue crack growth rates measured in gaseous hydrogen.

NOMENCLATURE

a	crack depth
B	thickness of compact tension specimen
c	one-half of the crack length at inner surface of vessel
da/dN	fatigue crack growth rate
F	function that describes crack size
K_{max}	maximum applied stress intensity factor
K_{min}	minimum applied stress intensity factor
ΔK	stress intensity factor range imposed during fatigue
L	length of cylindrical section of pressure vessel
p	hydrogen gas pressure
Q	geometric constant
r	radius of pressure vessel (average of inside and outside radius)
R	ratio of minimum to maximum applied load (or stress intensity factor)
t	wall thickness of pressure vessel
W	width of compact tension specimen
ξ	normalized crack length

1. INTRODUCTION

Steel pressure vessels are used to distribute a broad range of industrial gases, including gaseous hydrogen. Although hydrogen is known to reduce fatigue and fracture resistance of structural steels, the design rules for standard transportable pressure vessels are not specifically modified for containment of gaseous hydrogen in standards used predominantly in North America; e.g., vessels certified to US Department of Transportation (DOT) are the same for gaseous hydrogen as for inert gases. In some international standards, on the other hand, the tensile strength of the steels used in transportable pressure vessels is limited to <950 MPa. This limit was the outcome of laboratory study, which was motivated by a significant number of failures of hydrogen pressure vessels in Europe in the 1970s [1]. The observed failures were attributed to hydrogen-assisted fatigue of high-strength steels [1]. More recently, the American Society of Mechanical Engineers (ASME) has become the first to

codify pressure vessel design methodologies that accommodate the effect of gaseous hydrogen on fatigue crack growth rate (Boiler and Pressure Vessel Code, Section VIII, Division 3) [2].

In general, service history with hydrogen pressure vessels shows that the DOT design rules are adequate for common operating environments for transportable steel pressure vessels; other hydrogen pressure vessels have also been used successfully. The available service experience, however, appears to be insufficient to demonstrate the safety margin associated with cycle life on the order of ten thousand cycles and greater, since service experience is generally for low numbers of pressurization-depressurization cycles. As new applications are developed using gaseous hydrogen as a fuel, additional consideration of the effects of gaseous hydrogen are necessary for duty cycles that include higher pressure and greater number of pressurization cycles.

This work was motivated by the need to better understand the fatigue life of (Type 1) steel pressure vessels in applications where pressure vessels are cycled several times per day and >10,000 times over their lifetime. In particular, this work aims to support the development of new standards, such as Compressed Hydrogen-Powered Industrial Truck, On-board Fuel Storage and Handling Components (HPIT1) from CSA America. The scope of the testing was defined to address the conservative nature of fatigue life assessment based on fatigue crack growth as found in ASME BPVC Section VIII, Division 3. Additionally, the testing aims to inform methods of performance testing that use full-scale pressure vessel cycling to qualify pressure vessel designs. To meet these goals, a testing matrix was devised in collaboration with stakeholders from industry. This testing includes pressure cycling of full-scale, Type 1 pressure vessels with gaseous hydrogen, as well as materials evaluation in high-pressure gaseous hydrogen.

2. EXPERIMENTAL PROCEDURES

A closed-loop gas handling system was designed to pressure cycle a relatively large volume between pressure of about 43.8 MPa (6,350 psi) and 3.4 MPa (500 psi), using gaseous hydrogen as the working fluid. The pressurized volume consisted of up to ten pressure vessels in parallel. In order to minimize the volume of hydrogen required in the system, filler was used in the pressure vessels to reduce their free volume. The filler consisted of steel bearings and epoxy; a bladder was used to separate the filler mixture from the internal surface of the vessel. The steel bearings alone fill approximately 60% of the internal volume of the pressure vessels; the epoxy fills the majority of the remaining volume and prevents the steel bearing from settling as the tank expands under pressure. As the epoxy cures, it shrinks creating a small gap around the inside wall of the vessel.

The gas handling system consisted of a two-stage diaphragm compressor, high-pressure accumulators, the manifold connected to the volumes to be pressurized, and low-pressure accumulators. The low-pressure accumulators provide the source gas to the compressor, which continuously pressurizes the high-pressure accumulators. During the high-pressure end of the pressurization cycle, the compressor also directly pressurizes the pressure vessels. After the nominally static pressure hold on the pressure vessels, the hydrogen is vented to the low-pressure accumulators (i.e., the source volume).

The pressure cycle was designed to fill the pressure vessels over a period of about two minutes, hold the pressure in the vessels for about two minutes, then vent and hold the minimum pressure for about one minute, such that the total pressure cycle is approximately 5 minutes. Examples of the applied pressure cycles are shown in Figure 1. Initially, the system nominally followed cycle A in Figure 1. Early in the testing program, however, significant modifications to the gas handling system were necessary to insure continuous operation. These modifications rendered cycle A impossible to maintain and cycle B (Figure 1) become the nominal pressure cycle and has been used for the majority of cycling.

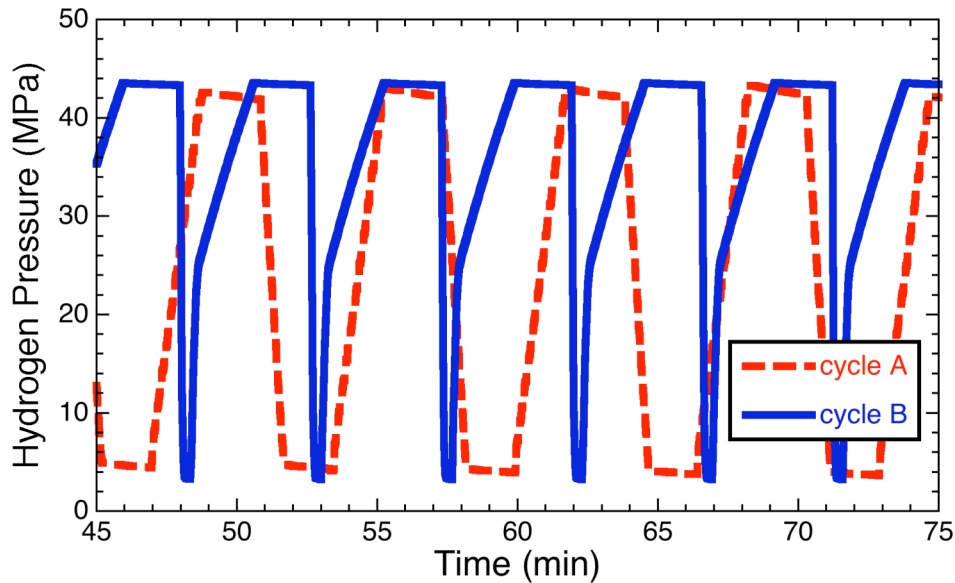


Figure 1. Hydrogen pressure cycles applied to the pressure vessels. Cycle A was applied during the initiation stages of testing; however, the majority of pressure cycles followed the cycle B profile.

Each pressure vessel to be tested was placed in a secondary vessel designed to contain the gaseous hydrogen upon failure. These secondary vessels were backfilled with nitrogen to a pressure slightly greater than ambient and each secondary is isolated from the vent manifold by a check valve. A pressure sensor on the secondary allows the pressure in each secondary to be monitored real-time, such that failure of any given pressure vessel could be identified by a rapid pressure increase.

Two pressure vessel designs were investigated in this study, and are referred to throughout as T1 and T2. Both types of pressure vessels were manufactured from Cr-Mo quench and tempered steel and are consistent with US Department of Transportation (DOT) design criteria for transportable pressure vessels (DOT 3AA designation from 4130X grade steel). The T1 design is a single-ended vessel with a flat bottom and hemispherical top. The T2 design is a double-ended vessel with ports at both hemispherical ends. The maximum hoop stress in the wall of the T2 design is slightly smaller than in the T1 design: <350 MPa in both cases.

Three pressure vessels of the T1 design were cycled in the as-manufactured condition, while a single vessel of the T2 design was cycled in the as-manufactured condition. In addition, engineered defects were machined on the internal surface of a number of pressure vessels prior to cycling. The engineered defects were produced prior to manufacturing the hemispherical ends by plunge electrodischarge machining. Ten defects were machined into each vessel: five equally spaced around the circumference nominally at distance of $L/3$ from one end of the cylindrical section (where L represents the length of the cylindrical section of the vessel) and five at an equivalent distance from the other end of the cylindrical section. The engineering defects were designed as semi-elliptical in shape with an aspect ratio ($a/2c$) of $1/3$ and a nominal root radius of 0.5 mm. These engineered defects were oriented such that the hoop stress drives cracking: the long axis of the defect is along the length of the vessel.

In general, all ten defects in given vessel were intended to be equivalent. In a few pressure vessels, engineered defects of two sizes were machined, five of each of size. The engineered defects were designed to represent specific values of ΔK at the beginning of cycling (and assuming a sharp crack) when cycled between pressure of approximately 43.8 MPa (6,350 psi) and 3.5 MPa (500 psi). The engineered defects represented ΔK values approximately in the range from 11 and 20 MPa $m^{1/2}$. In addition, the aspect ratio of the engineered defects was varied in one pressure vessel (T1-11), while keeping the ΔK nominally constant at 12 MPa $m^{1/2}$: in this vessel, five defects were designed with an

aspect ratio ($a/2c$) of 1/12 and the other five with an aspect ratio of 1/2. Table 1 summarizes the pressure vessels and their engineered defects.

Table 1. Pressure vessel designations and engineered defect designations. The aspect ratio ($a/2c$) of the engineered defects is 1/3, with the exception of pressure vessel T1-11, which contains engineered defects with aspect ratios of 1/2 and 1/12.

Pressure vessel designation	Engineered defect designation	Nominal ΔK (MPa m ^{1/2})	Number of engineered defects
T1-01			
T1-02	As-manufactured	n/a	n/a
T1-03			
T1-05	B	12	10
T1-06	B	12	10
T1-07	F	20	10
T1-08	F	20	10
T1-09	A	11	5
	C	13	5
T1-10	D	16	5
	E	18	5
T1-11	B-2	12	5
	B-12	12	5
T2-01	As-manufactured	n/a	n/a
T2-02	A	11	5
	C	13	5
T2-04	F	20	10

After a pressure vessel had failed, the location of the through-wall crack could not be distinguished from general superficial damage on the external surface of the pressure vessel due to routine handling. The location of the critical crack was identified by wrapping the pressure vessel with tape and pressurizing with an inert gas. As gas escapes through the crack, a blister under the tape identifies the location of the crack. With this crack as the reference point, panels were sectioned from the pressure vessel for each of the engineered defects. The panels were broken open at the engineered defect by cooling to liquid nitrogen temperature and loading in three-point bending.

Fracture mechanics tests were performed on three heats of 4130X quench and tempered steel. Specimens were machined from manufactured pressure vessels or from equivalently processed test rings. All materials had tensile strength <950 MPa. Heat N represents the T1 pressure vessels; specimens were machined directly from a sectioned pressure vessel. The other heats represent vessels that were not tested in this study. Fatigue crack growth tests were performed in gaseous hydrogen at pressure of 45 MPa, following the guidance of ASTM E647. Details of the testing specific to testing in gaseous hydrogen are given in Refs. [3, 4]. Compact tension specimens were machined with thickness (B) of 12.7 mm, such that the cracks propagate along the axis of the pressure vessel on the same fracture plane as a through-wall crack; this is the CL orientation with respect to the cylindrical pressure vessel (the engineered defects in the pressure vessels propagate cracks in the CR orientation). The width of the specimen (W) is 26.4 mm. The thickness was reduced along the crack plane by side grooves (45° V-groove): nominal reduction of 12% and root radius of nominally 0.5 mm for fatigue crack growth tests.

Constant load amplitude, fatigue crack growth tests were performed at frequency of 1 Hz and R -ratio of 0.1 ($R = K_{min}/K_{max}$). Precracking was performed in air, shedding load to a K_{max} of <10MPa m^{1/2} at the end of precracking (initial fatigue loads were greater than the final maximum precracking load).

The relative crack position (a/W) at the beginning of fatigue crack growth testing was 0.27 to 0.29. The K_{max} at the end of fatigue testing was typically less than $30 \text{ MPa m}^{1/2}$.

3. RESULTS

3.1 Materials Characterization

The fatigue crack growth rates of the three heats of steel are shown in Figure 2 for $R = 0.1$ and frequency of 1 Hz in gaseous hydrogen at pressure of 45 MPa. The fatigue crack growth rate of heat C was previously reported in Ref. [4]. All three heats of 4130X show essentially the same fatigue crack growth rates in gaseous hydrogen for ΔK in the range of 10 to 20 $\text{MPa m}^{1/2}$. The fracture resistance of heat C in gaseous hydrogen at pressure of 45 MPa is reported to be in the range of 50 to 70 $\text{MPa m}^{1/2}$ [4]. The fracture resistance of heat N was not measured. For heat P, crack extension during fracture resistance testing was extremely non-uniform across the thickness of the specimen; thus, it is not reported here.

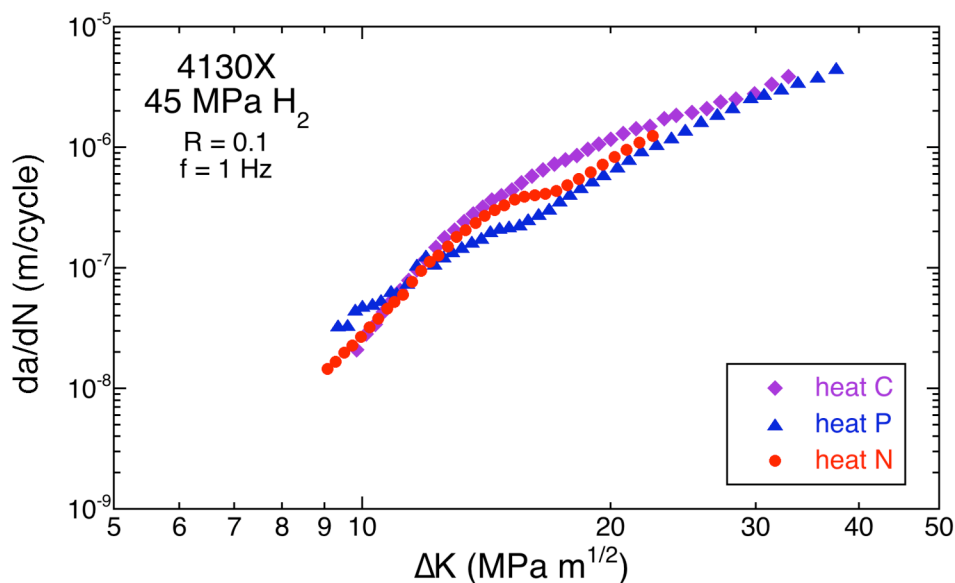


Figure 2. Fatigue crack growth rates for three heats of 4130X pressure vessel steels.

3.2 Pressure Vessel Cycling

The status of cycling at the time of writing is summarized in Figure 3; the arrows indicate pressure vessels that are still being cycled. Each of the three as-manufactured T1 pressure vessels have experienced $>35,000$ cycles without failure, while the single, as-manufactured T2 pressure vessel has been subjected to $>16,000$ cycle without failure. Pressure vessels of both designs with the deepest engineered defect (F, initial $\Delta K \sim 20 \text{ MPa m}^{1/2}$) failed after 8,048 and 14,329 cycles (T1-07 and T2-04, respectively). Additionally, pressure vessel T1-10 failed after 15,020 cycles at a type D engineered defect that was improperly machined to a significantly greater depth than designed. Incidentally, all other engineered defects that have been examined show nominal dimensions that are consistent with their design, with the exception that the root radius is about 50% greater than specified. Generally, the bladder successfully contained the epoxy with one exception: epoxy was found embedded in the engineered defect that initiated failure of T1-07.

In all three failures, the pressure vessels failed gracefully by leaking at a through-wall crack during the pressurization stage of the pressure cycle. Figure 4 shows the two cycles just prior to failure of one of the pressure vessels. Clearly, the defect becomes a through-wall crack during the pressurization stage and not during the high-pressure hold (or some other stage in the pressure cycle). The pressure vessel

volumes slowly leak through the stable crack until the pressure system stops due to low-pressure detected in the accumulators. The leak rate through the crack was estimated to be approximately 1.5 kg/hr (0.42 g/s) based on the initial pressure rise in the secondary vessel (and assuming that the gas in the secondary remains isothermal at ambient temperature).

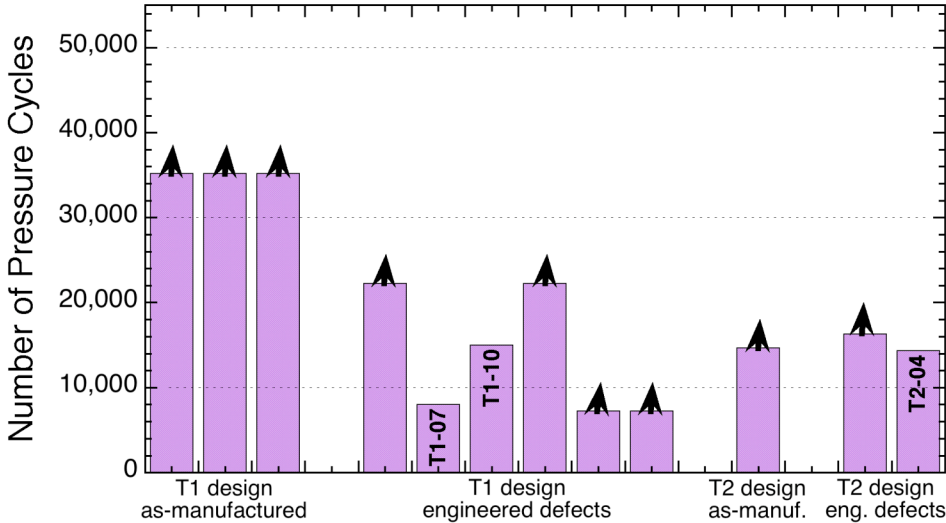


Figure 3. Number of pressure cycles for each group of tests. Arrows indicate pressure vessels that are still cycling. The pressure vessels that failed are noted by the pressure vessel designation.

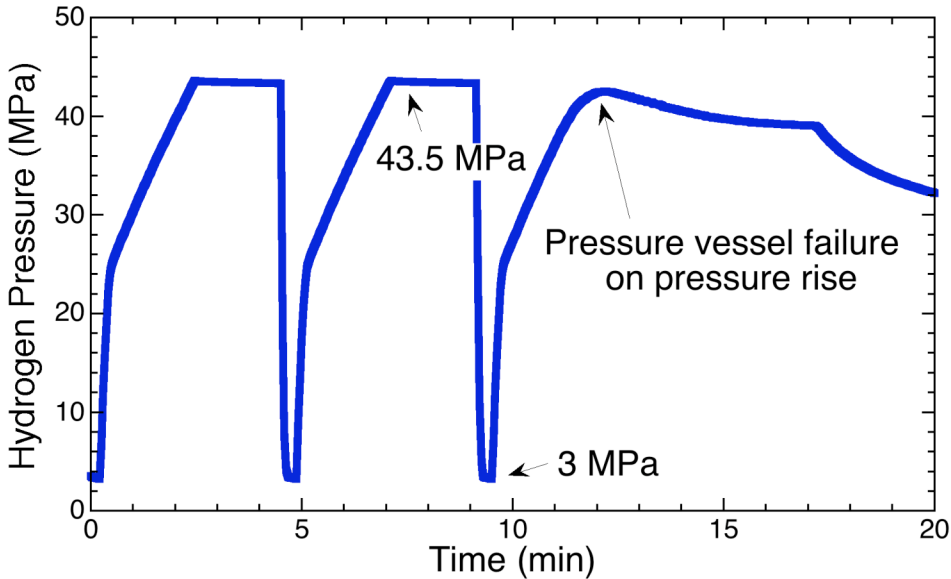


Figure 4. Hydrogen pressure cycles just prior to failure of T1-07. The transition at approximately seventeen minutes corresponds to a valve closure isolating the pressure vessels from the compressor.

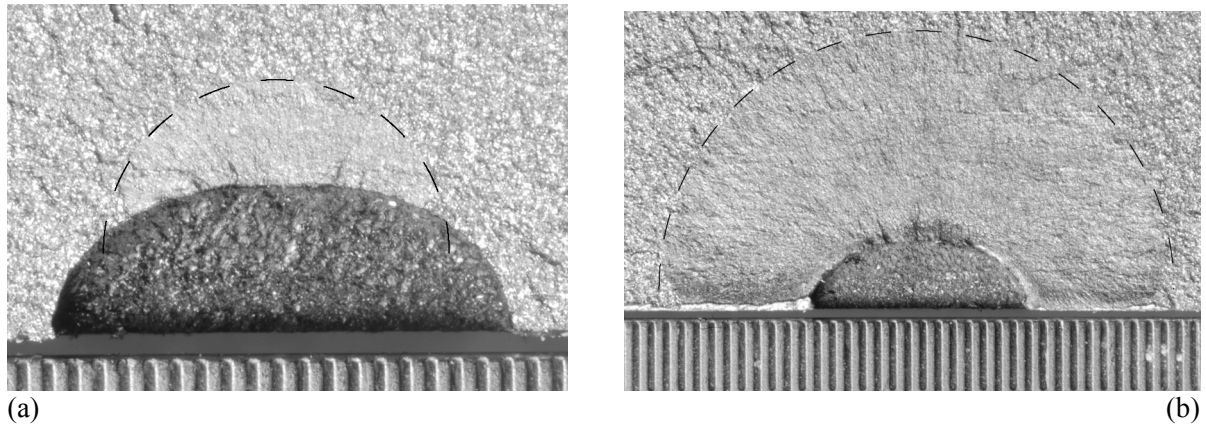


Figure 5. Crack extension from engineering defects that did not extend through the thickness of the pressure vessel, showing semicircular crack extension (outlined by dashed profile): (a) T1-07, crack extension of ~ 1 mm and (b) T1-10, crack extension of greater than 3 mm. The ruler marks are 0.25 mm (0.01 in) apart.

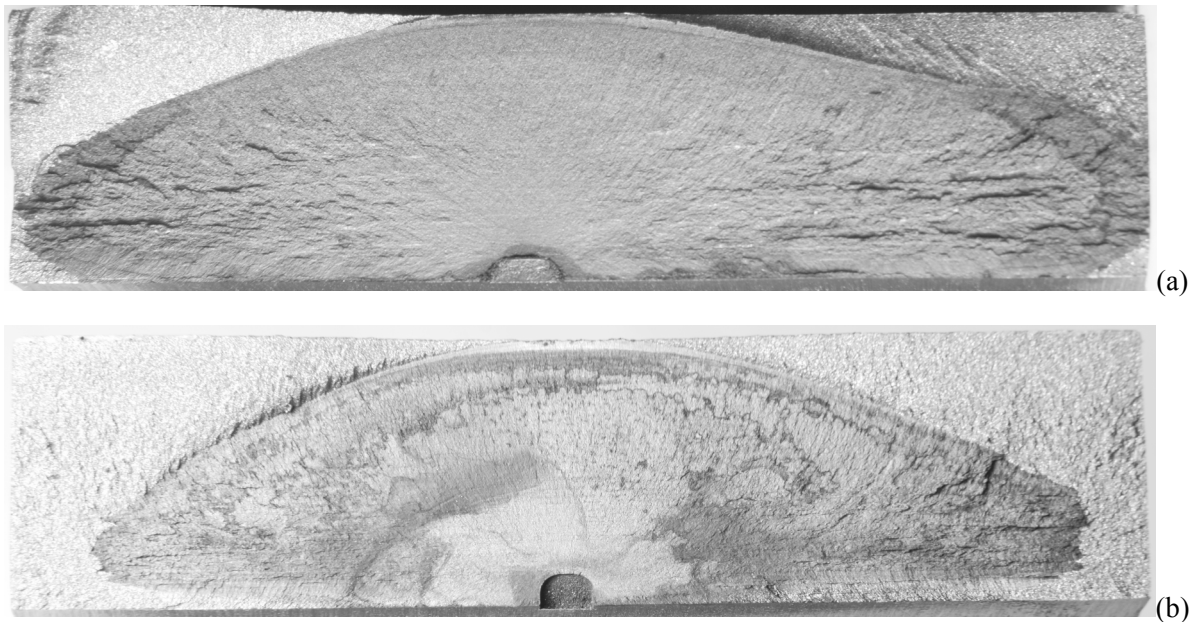


Figure 6. Through-wall cracks associated with the engineered defects do not have a semicircular crack profile: (a) T1-07, (b) T1-10. The dark shading is the result of rust formation during sectioning of the defect panels. Note also that the defect in T1-10 was machined significantly deeper than designed, which accounts of the shape of the defect.

3.3 Microscopy

All engineered defects in the failed T1 pressure vessels that have been evaluated (16 of 20) have shown crack propagation. In general, crack extension in the T1 vessels is small (<1 mm) with the exception of the engineered defect that led to failure. Cracks extend from the deepest extent of the engineered defects with a nominally semi-circular profile (Figure 5). This is shown most dramatically in one defect from T1-10 (Figure 5): this defect grew to a depth of several millimeters, clearly with a semi-circular profile. The cracks that caused failure are not semi-circular, rather they extend along the center of the wall thickness, as shown in Figure 6.

High-resolution imaging of the fracture surfaces from the T1 failures show that fracture is predominately transgranular (Figure 7). Secondary cracking is observed orthogonal to the primary

crack extension direction. The roughness of the cracks increases as the cracks extend perpendicular to the through-wall direction, although qualitatively the fracture features are similar over the entire hydrogen fracture surface. A few isolated regions of intergranular failure were observed in bands that appear to be aligned parallel to the wall, and do not follow the contour of the crack.

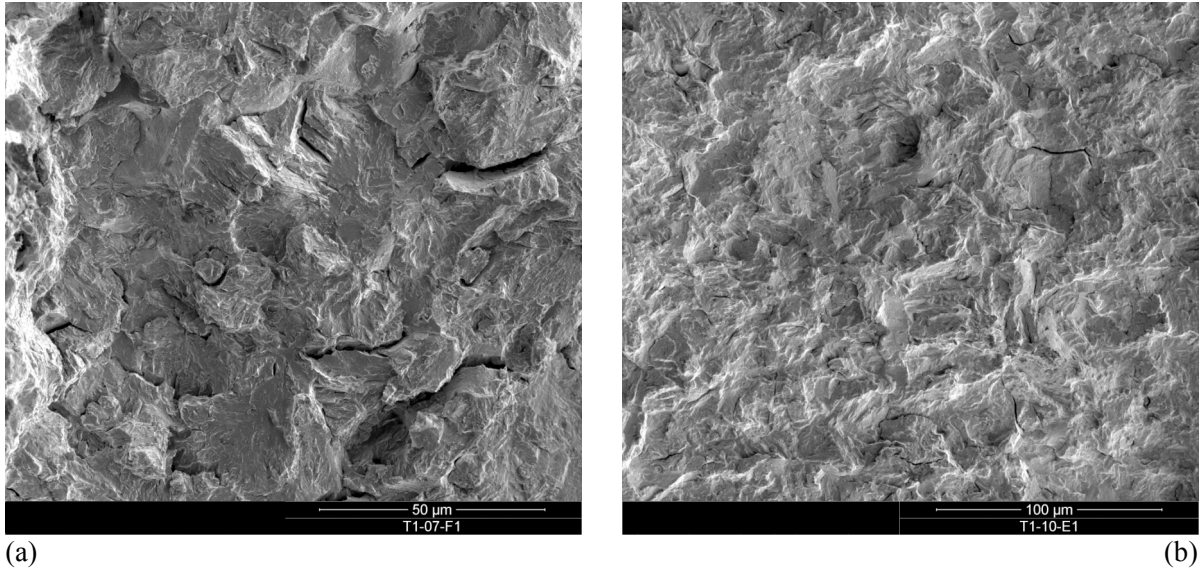


Figure 7. Scanning electron micrographs of fatigue fracture ahead of engineered defects for (a) T1-07 and (b) T1-10.

3.4 Estimates of Fatigue Crack Growth

The number of cycles to propagate a crack through the wall thickness can be estimated, provided that a number of important assumptions are made. The crack is assumed to propagate based on the ΔK - da/dN relationship measured from compact tension specimens. It is assumed that crack maintains a semi-circular crack shape ($a/2c = 1/2$) from initiation to propagation through wall. This aspect ratio is different from that of the machined defects, but reflects the shape of the propagating cracks. The driving force (ΔK) for crack extension is represented by the relationships from Anderson [5] over the whole range of crack extension. Anderson gives the driving force for a part-through internal defect of finite length as:

$$\Delta K = (p_{\max} - p_{\min}) \left(\frac{r}{t} \sqrt{\frac{\pi a}{Q}} \right) F \quad (1)$$

where p_{\max} and p_{\min} are the maximum and minimum pressure during cycling, r is the average of the inside and outside radius of the vessel wall, t is the wall thickness of the pressure vessel, Q is a geometric constant equal to 2.4640 for a semicircular crack, and F is a functional form that describes the size of the crack as

$$F = 1.12 + 0.053\xi + 0.0055\xi^2 + \left(1 + 0.02\xi + 0.0191\xi^2 \right) \frac{\left(20 - \frac{r}{t} \right)^2}{1400} \quad (2)$$

with the normalized crack length (ξ) equal to

$$\xi = \frac{2c}{t} \quad (3)$$

Although these relationships are only valid for $a/t < 0.8$, the calculations are applied for crack depth (a) from the initial depth of the engineered defect until the crack as propagated through the full wall thickness ($a = t$). The calculated number of cycles to propagate the crack the final 20% of the wall thickness is generally small, less than about 7% of the total number of cycles to through-wall penetration. The crack depth (a) as a function of cycle number (N) is determined by numerical integration according to

$$a_{i+1} = a_i + \left. \frac{da}{dN} \right)_i \Delta N \quad (4)$$

where

$$\left. \frac{da}{dN} \right)_i = C(\Delta K_i)^m \quad (5)$$

C and m are constants. The relationships between ΔK and da/dN from Ref. [4] for heat C are adopted for these calculations over the entire range of crack propagation; the values of C and m are given in Table 2 for specific ranges of ΔK . The number of cycles to failure for each initial defect depth is given in Figure 8, along with the estimated time to growth the crack from the initial machined defect to a through-wall crack.

Table 2. The fatigue crack growth constants for AISI 4130 steel in gaseous hydrogen at pressure of 45 MPa. Values at low ΔK ($< 7.6 \text{ MPa m}^{1/2}$) are generic values for high-strength low alloy steels in air; data in gaseous hydrogen are extrapolated to the relationship in air at low values of ΔK .

ΔK (MPa m ^{1/2})	C (m/cycle)	m	Ref.
$\Delta K < 7.6$	3.64×10^{-12}	3.26	[6]
$7.6 \leq \Delta K < 14$	1.05×10^{-16}	8.41	[4]
$14 \leq \Delta K < 20$	3.87×10^{-11}	3.44	[4]
$\Delta K \geq 20$	1.45×10^{-9}	2.24	[4]

4. DISCUSSION

The pressure cycle for the full-scale testing was designed to maximize test efficiency, while minimizing the effects of the frequency of the pressure cycles. A general trend suggests that the fatigue crack growth increment per cycle (da/dN) increases as the frequency is decreased; however, this trend cannot extend to infinitely small frequency. For ferrite steels exposed to gaseous hydrogen at pressure comparable to the pressure used in this study, fatigue crack growth rates approach a plateau value at frequency below 1 to 0.1 Hz [7]; others have reported no difference in fatigue crack growth rate in this range of frequency for pipeline steels at lower pressure [8]. In the case of higher hydrogen gas pressures and very high-purity gas, the fatigue crack growth rate is reported to modestly increase as the frequency is reduced to about 0.001 Hz [9]. Hold times at the peak of the cycle may increase crack growth rate when the frequency is quite high; however at lower frequency, the rate of loading is particularly important, while long hold times may retard fatigue crack growth [7, 9]. Based on this available data, the pressure cycle was designed to balance conservative testing rates with the practicality of conducting the tests, resulting in the five-minute pressure cycle, which corresponds to a frequency of approximately 0.003 Hz.

The observed failure mode of the pressure vessels is an important outcome of this study. For each failed pressure vessel, the failure occurred during pressurization and not during the hold time at peak pressure. This observation is consistent with fracture mechanics test observations [10] as well as service history of hydrogen containing pressure vessels [11]. This result can also be anticipated from fracture testing of low-strength, ductile steels [12] and suggests that the cracks are relatively stable at the peak pressure. Additionally, cracks propagated until a leak prevented maintaining pressure in the vessel without rupture of the vessel. Although service conditions may be substantially different for these pressure vessels compared to the testing environment (e.g., in the field, these pressure vessels would not be filled with steel bearings and epoxy), the observed leak-before-burst mode of failure is an important safety consideration for the design of hydrogen pressure vessels.

From a performance perspective, the tested pressure vessels behave as might be expected of relatively ductile steels. To date, the as-manufactured T1 vessels have not failed after >35,000 cycles, while the as-manufactured T2 vessel has experienced almost 15,000 cycles. These results are consistent with the work of Kesten and Windgassen on pressure cycling of similar vessels: failure due to cycling in gaseous hydrogen was not observed for hoop stresses less than about 400 MPa when no apparent surface defects were present [13]; maximum hoop stress in these tests is <350 MPa. Failures, however, were observed by Kesten and Windgassen at lower stresses in a few instances where “hardly visible” surface defects could be found [13].

Defects and surface irregularities are unavoidable in a manufacturing setting and difficult to characterize. In general, defects of a predetermined size are cause to reject a pressure vessel; moreover, inspection in a manufacturing setting is often based on a comparative measure, not necessarily quantitative characterization of the defect. The effectiveness of a defect at extending a fatigue crack, for example, depends on several factors, such as the acuteness (or sharpness) of the defect, and not just the depth of the defect. Thus, pressure cycling of a relatively small number of vessels cannot provide quantitative evaluation of all manufacturing processes or all families of potential defects.

The engineered defects were designed to introduce nominally known defects of various sizes into the pressure vessels with the goal of providing additional information about defect sizes. The depth of these defects ranged from a few percent to about 10% of the nominal wall thickness, thus spanning common inspection limits. Because the two pressure vessels that were examined have different wall thickness, the engineered defects were normalized to achieve a specific ΔK during pressure cycling (Table 1). The deepest engineered defects (highest ΔK) resulted in failure after 8,000 to 14,000 cycles depending on the details of the vessel design. Smaller (but still visible) defects have cycled for significantly greater number of cycles and these vessels continue to be pressure cycled (Figure 3). In any case, the number of cycles to failure are significantly greater than reported by Kesten and Windgassen for similar ΔK [14]. Kesten and Windgassen showed that the cycle life depended on the “sharpness” of the engineered defect [14], however, the root radius of the engineered defects in this study are consistent with the smallest root radius (sharpest defects) in the Kesten and Windgassen study. Additionally, Kesten and Windgassen report intergranular fracture as a significant fracture mode in their steels [13], which is a fracture mode typically associated with low resistance to fracture. Although it was observed in this study, intergranular failure did not appear to dominate the fracture process in these investigations, suggesting differences in the quality of the steels tested by Kesten and Windgassen (although admittedly, the scarcity of testing details from the Kesten and Windgassen studies make comprehensive comparisons difficult).

An additional aim of the present study is comparison of full-scale tests with engineering analysis as shown in Figure 8. The engineering analysis method (shown in Figure 8) provides conservative estimates of cycle life since it considers only the number of cycles to propagate an existing crack and does not account for the period of time to initiate a propagating crack from the comparatively blunt machined defects. The initiation period can be idealized as the difference between the predicted cycles to failure (curves in Figure 8) and the actual cycles to failure (symbols in Figure 8) and can be expected to vary for defects with different shapes and sharpness. These results suggest that the number

of cycles to initiate a growing crack from the machined defects represents one-half to two-thirds the total cycles to failure. While this is consistent with previous reports [15], there are many assumptions in the calculations shown in Figure 8. For example, the crack is assumed to grow with a semicircular profile through the entire wall thickness, which is neither correct at the beginning of crack extension (Figure 5a), nor at the end of life (Figure 6). Nevertheless, the engineering analysis method is clearly shown to be conservative for these engineered defects. Thus, the engineering analysis method may be used to conservatively determine the necessary inspection limit for a desired lifetime. A desired lifetime of 10,000 cycles corresponds to the number of cycles required to propagate a sharp, semicircular, crack-like defect from an initial depth in the range of 0.5 to 0.7 mm to failure.

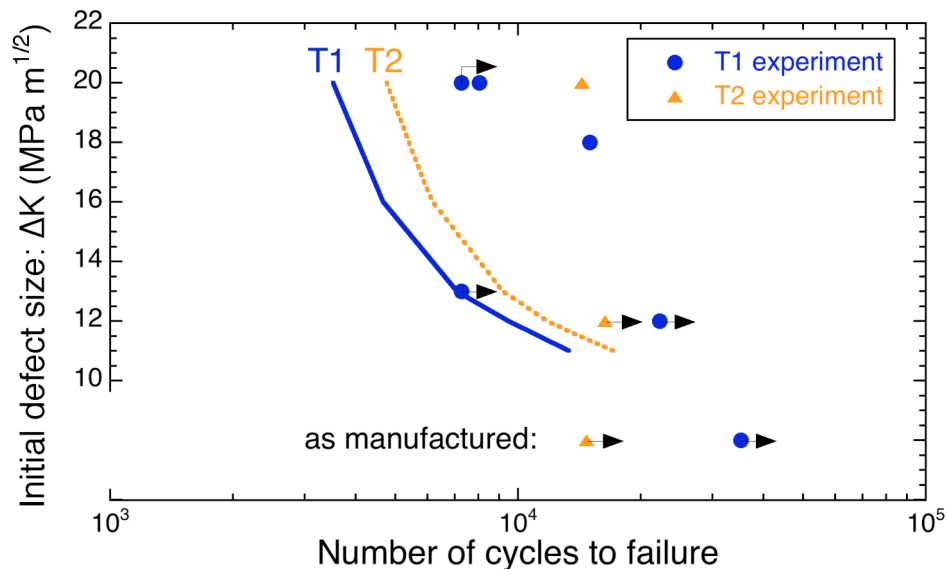


Figure 8. The number of cycles to failure in the cycled pressure vessels are given by the symbols; arrows indicate that the pressure vessel was still cycling at the time of writing. The curves represent the estimated cycles to propagate the initial defect to a through-wall crack.

5. SUMMARY

Full-scale Type 1 pressure vessels are being cycled with gaseous hydrogen. The results to date on hydrogen-assisted fatigue and fracture of pressure vessels suggest that pressure vessels from low-strength Cr-Mo steels (tensile strength <900 MPa) have lifetimes greater than 30,000 cycles. Engineered defects machined into the inside surface of the pressure vessels significantly reduces the number cycles to failure; however, the measured cycles to failure are significantly greater than the cycles to failure predicted by engineering analysis using measured fatigue crack growth rates for long cracks in gaseous hydrogen. Pressure cycling of vessels continues at the time of writing and more comprehensive analysis of these results is expected in the future.

ACKNOWLEDGEMENTS

Sandia National Laboratories is a multi-program laboratory managed and operated by Sandia Corporation, a wholly owned subsidiary of Lockheed Martin Corporation, for the U.S. Department of Energy's National Nuclear Security Administration under contract DE-AC04-94AL85000.

REFERENCES

1. RS Irani. Hydrogen storage: high-pressure gas containment. *MRS Bulletin* 27 (2002) 680-682.
2. MD Rana, GB Rawls, JR Sims and E Uptis. Technical basis and application of new rules on fracture control of high pressure hydrogen vessel in ASME Section VIII, Division 3 code (PVP2007-26023). in: *Proceedings of Pressure Vessels and Piping Division Conference, 2007*, San Antonio TX. American Society of Mechanical Engineers.
3. C San Marchi, BP Somerday, KA Nibur, DG Stalheim, T Boggess and S Jansto. Fracture and fatigue of commercial grade pipeline steels in gaseous hydrogen (PVP2010-25825). in: *Proceedings of PVP-2010: ASME Pressure Vessels and Piping Division Conference, 2010*, Bellevue WA. American Society of Mechanical Engineers.
4. KA Nibur, C San Marchi and BP Somerday. Fracture and fatigue tolerant steel pressure vessels for gaseous hydrogen (PVP2010-25827). in: *Proceedings of Pressure Vessels and Piping Division Conference, 2010*, Bellevue WA. American Society of Mechanical Engineers.
5. TL Anderson. *Fracture Mechanics: Fundamentals and Applications (Second Edition)*. Boca Raton FL: CRC Press (1995).
6. Article KD-4, *Fracture Mechanics Evaluation*. ASME Boiler and Pressure Vessel Code, Section VIII, Division 3. American Society of Mechanical Engineers, 2009.
7. P McIntyre, PH Pumphrey and DJ Goddard. The influence of high pressure hydrogen gas on the rate of fatigue crack growth in pressure vessel steel to BS1501-224 Grade 32B – Final Report (R21.63.5). Central Electricity Generating Board, 1984.
8. HJ Cialone and JH Holbrook. Effects of gaseous hydrogen on fatigue crack growth in pipeline steel. *Metall Trans* 16A (1985) 115-122.
9. RJ Walter and WT Chandler. Cyclic-load crack growth in ASME SA-105 grade II steel in high-pressure hydrogen at ambient temperature. in: AW Thompson and IM Bernstein, editors. *Effect of Hydrogen on Behavior of Materials*. *Proceedings of an International Conference (Moran WY, 1975)*. The Metallurgical Society of AIME, 1976. p. 273-286.
10. RP Gangloff. Science-based prognosis to manage structural alloy performance in hydrogen. in: BP Somerday, P Sofronis and R Jones, editors. *Effects of Hydrogen on Materials*. *Proceedings of the 2008 International Hydrogen Conference (Moran WY, 2008)*. ASM International, 2009. p. 1-21.
11. RS Irani. Hydrogen embrittlement: How it was resolved in the 1980s. presentation from: ISO TC58/WG7, Gas Cylinder Compatibility, Atlanta GA, 29 September 2008.
12. KA Nibur, BP Somerday, C San Marchi, JWI Foulk, M Dadfarnia, P Sofronis and GA Hayden. Measurement and interpretation of threshold stress intensity factors for steels in high-pressure hydrogen gas (SAND2010-4633). Sandia National Laboratories, Livermore CA, 2010.
13. M Kesten and K-F Windgassen. Hydrogen-assisted fatigue of periodically pressurized steel cylinders. in: IM Bernstein and AW Thompson, editors. *Hydrogen Effects in Metals*. *Proceedings of the Third International Conference on Effect of Hydrogen on Behavior of Materials (Moran WY, 1980)*. The Metallurgical Society of AIME, 1981. p. 1017-1025.
14. M Kesten and AL Window. Design of equipment to resist hydrogen fatigue service. in: CG Interrante and GM Pressouyre, editors. *Proceedings of the First International Conference on Current Solutions to Hydrogen Problems in Steels*, Washington DC. American Society for Metals, 1982.
15. M Kesten and P Runow. On the kinetics of environmentally assisted fatigue cracking of pressure vessel steels in the presence of hydrogen gas. in: *Metallic Corrosion: Proceedings of the 8th International Congress on Metallic Corrosion*, Mainz, Germany. Dechema, 1981. p. 420-425.